Colloid Polym Sci (2005) 283: 504–511
DOI 10.1007/s00396-004-1215-z

ORIGINALCONTRIBUTION

Kabir-ud-Din
S. M. Shakeel Iqubal
Zaheer Khan

Reduction of soluble colloidal MnO_2 by DL-malic acid in the absence and presence of nonionic TritonX-100

Received: 9 June 2004
Accepted: 4 September 2004
Published online: 1 December 2004

Kabir-ud-Din (✉) · S. M. S. Iqubal
Department of Chemistry,
Aligarh Muslim University,
Aligarh, 202 002, India
E-mail: kabir7@rediffmail.com
Tel.: +91-571-2703515

Z. Khan
Department of Chemistry,
Jamia Millia Islamia, Jamia Nagar,
New Delhi, 110 025, India

Abstract Kinetics of oxidation of DL-malic acid by water soluble colloidal MnO_2 (prepared from potassium permanganate and sodium thiosulfate solutions) have been studied spectrophotometrically in the absence and presence of nonionic Triton X-100 surfactant. The reaction is autocatalytic and manganese(II) (reduction product of the colloidal MnO_2) may be the autocatalyst. The order of the reaction is first in colloidal [MnO_2] as well as in [malic acid] both in the absence and presence of the surfactant. The reaction has acid-dependent and acid-independent paths and, in the former case, the order is fractional in [H^+]. The effect of externally added manganese(II) is complex. The results show that the rate constant increases as the manganese(II) concentration is increased. It is not possible to predict the exact dependence of the rate constants on manganese(II) concentration, which has a series of reactions with other reactants. In the presence of TX-100, the observed effect on k_ψ is catalytic up to a certain [TX-100]; thereafter, an inhibitory effect follows. The catalytic effect is explained in terms of the mathematical model proposed by Tuncay et al. (in Colloids Surf A Physicochem Eng Aspects 149:279 3). Activation parameters associated with the observed rate constants (k_{obs}/k_ψ) have also been evaluated and discussed.

Keywords Colloidal MnO_2 · DL-Malic acid · Kinetics · Surfactant · Triton X-100

Introduction

Perez-Benito et al. [1, 2] reported the oxidation of formic and oxalic acids by water soluble colloidal MnO_2 and these studies were extended by Tuncay et al. [3] and Kabir-ud-Din et al. [4] to micellar media. In case of lactic acid oxidation by colloidal MnO_2, it was observed that the process took place in two steps [5] (nonautocatalytic and autocatalytic) and that the second step disappeared completely in the presence of added manganese(II). We see that the above cited papers [3, 4] are the only few concerned with the effect of surfactant on the redox chemistry of colloidal MnO_2 [3, 4] while anionic-, cationic- and nonionic micellar effects on the kinetics and mechanism of organic and inorganic reactions have so far been extensively studied [6–12].

The oxidation of α-hydroxy acids has been particularly interesting because both C–H and C–C cleavage have been reported [13–15]. Recently [16], we have reported the oxidation of citric acid by colloidal MnO_2 that proceeded through the C–H and C–C bonds cleavage. We searched for another closely related system, where there is a possibility of C–C and C–H bond breaking, and such a situation is present in DL-malic acid. Therefore, in this paper we wish to report the results of investigations of the MnO_2 oxidation of

DL-malic acid both in the absence and presence of nonionic TX-100.

Experimental

Materials

Potassium permanganate (E. Merck, India, 98.5%), sodium thiosulfate (s.d.fine, India, 99%), perchloric acid (E. Merck, India, 70% solution), manganese(II) sulfate-1-hydrate (E. Merck, India, 99%), Triton X-100 (Fluka, Switzerland, 99%) and DL-malic acid (s.d. fine, India, 99%) were commercial products and were used as supplied. Water (deionized and CO_2 free) was used as the solvent after double distillation (first time from alkaline $KMnO_4$).

Preparation of water soluble colloidal MnO_2

For the preparation of colloidal MnO_2, standardized $KMnO_4$ ($= 5.0\times10^{-4}$ mol dm^{-3}) and sodium thiosulfate ($= 1.87\times10^{-4}$ mol dm^{-3}) were used to prepare the stock solution ($=5.0\times10^{-4}$ mol dm^{-3}—the reaction takes place in 8:3 ratio [1–5, 16]). The resulting solution was dark brown and perfectly transparent, which showed one broad band covering the whole visible region of the spectrum with λ_{max} = 390 nm (Fig. 1). The solution remained stable for several weeks. The colloidal particles of MnO_2 are known to be roughly spherical with a radius of about 500 Å [1, 3].

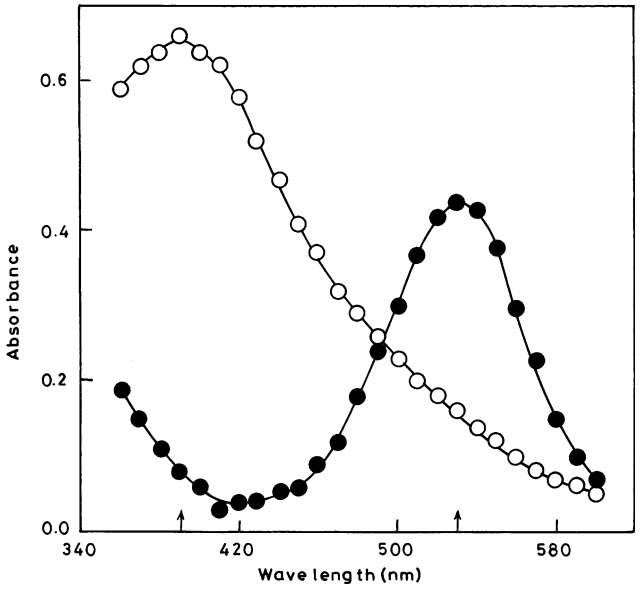

Fig. 1 Absorption spectra of $KMnO_4$ (1.6×10^{-4} mol dm^{-3}) and of the reaction product of $KMnO_4$ (8.0×10^{-5} mol dm^{-3}) and $Na_2S_2O_3$ (3.0×10^{-5} mol dm^{-3})

Kinetic measurements

The oxidation of DL-malic acid was carried out under pseudo-first-order conditions with at least a tenfold excess of reductant over oxidant concentration. The progress of the reaction was monitored spectrophotometrically by following the disappearance of the colloidal MnO_2 at 390 nm. The values of pseudo-first-order rate constants (k_{obs} or k_ψ, s^{-1}—k_{obs} refers to pure aqueous whereas k_ψ refers to aqueous-micellar media) were determined from the slope of plots of log(absorbance) versus time. The reaction was usually followed up to not less than 80% completion. The rate constants were reproducible within ±5%.

Results and discussion

The reaction was studied as a function of [MnO_2], [malic acid], and temperature both in the absence and presence of nonionic TX-100 micelles. Good first-order plots were obtained in all the kinetic experiments in which an excess of DL-malic acid (the reductant) over MnO_2 (the oxidant) was used. Tables 1, 2, 3, and 4 and Figs. 1, 2, 3, 4, 5, 6, and 7 record the results for different experimental conditions.

Reaction-time curve

Figure 2 shows the examples of the kinetic curves from which the k_{obs} for the oxidation were obtained. By inspecting Fig. 2, it is clear that the oxidation kinetics proceed in two steps, i.e., nonautocatalytic (initial slow) path followed by a relatively faster step (autocatalytic). The plots were linear up to ca. 40 min and, as the time increased from 40 min onward, deviations from linearity were observed. The time at which the deviation commenced was found to depend upon the [malic acid], [MnO_2], and temperature.

Rate dependence on [MnO_2]

The oxidation of DL-malic acid by MnO_2 was studied as a function of [MnO_2] between 2.0×10^{-5} and 10.0×10^{-5} mol dm^{-3} at constant [malic acid] ($=16.0\times10^{-4}$ mol dm^{-3}) at 30 °C. We see (Table 1) that the k_{obs} values decrease with increase in [MnO_2]. These observations are against the norms of kinetics (the pseudo-first-order rate constants should be independent of the initial concentration of the reactant in defect). Such type of behavior may be due to flocculation of the colloidal particles. In order to suppress any possible flocculation, the experiments were repeated in presence of gum arabic (a good

Table 1 Pseudo-first-order rate constants for the reaction of colloidal MnO_2 and DL-malic acid in the absence and presence of TX-100 (= 15.0×10^{-3} mol dm^{-3}) at 30 °C

10^5 [MnO_2] (mol dm^{-3})	Gum arabic (g dm^{-3})	10^4 [malic acid] (mol dm^{-3})	Aqueous		TX-100	
			10^4 k_{obs1} (s^{-1})	10^4 k_{obs2} (s^{-1})	10^4 $k_{\psi1}$ (s^{-1})	10^4 $k_{\psi2}$ (s^{-1})
2.0	0.0	16.0	4.6	7.2	5.6	8.0
3.2			4.8	6.8	5.4	6.7
4.0			4.3	6.1	5.0	6.1
4.8			3.2	6.0	4.8	5.8
6.0			3.1	5.7	4.6	5.6
7.2			2.9	4.7	4.4	5.4
8.0			2.9	4.6	4.3	5.2
8.8			2.7	4.4	4.1	5.1
10.0			1.9	4.3	3.8	4.8
8.0	0.0	16.0	2.9	4.6	4.3	5.2
		24.0	5.3	7.7	7.3	10.1
		32.0	6.7	11.2	9.1	11.6
		40.0	7.8	11.5	10.8	13.4
		48.0	11.0	16.0	11.8	14.5
		52.0	–	–	13.3	16.3
		56.0	11.8	17.6	–	–
		64.0	13.3	19.6	–	–
	1.0		3.3	Not observed		
	2.0		3.0	Not observed		
	3.0		2.9	Not observed		
	4.0		2.6	Not observed		
	5.0		2.4	Not observed		
	6.0		2.3	Not observed		

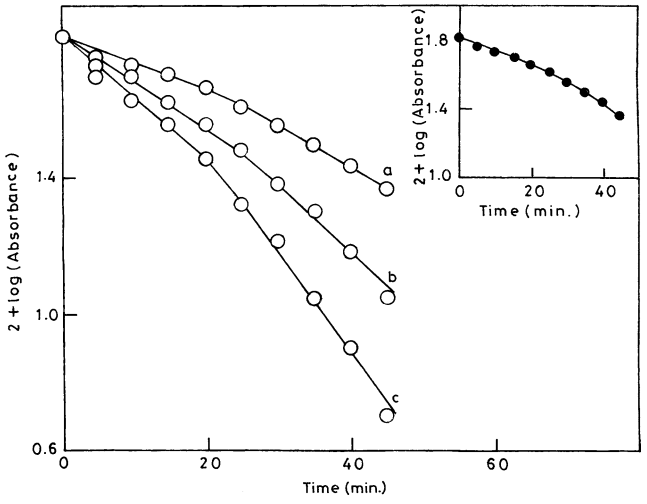

Fig. 2 Plots of log(absorbance) versus time for the reduction of colloidal MnO_2 by DL-malic acid. *Reaction conditions*: [MnO_2] = 8×10^{-5} mol dm^{-3}, [malic acid] = 16 (**a**), 24 (**b**), 56×10^{-4} mol dm^{-3} (**c**), temperature = 30 °C. *Inset* plot of log(absorbance) versus time for curve (**a**)

water-soluble polysaccharide known to stabilize colloidal MnO_2 [17]). Comparison between the k_{obs} obtained in the absence and presence of gum arabic (Table 1) suggests that no improvement is observed. Such type of behavior has earlier been observed in many oxidation reactions of organic oxidants by permanganate [18]. On the other hand, in the presence of gum arabic, there seems to be competition between the oxidant (DL-malic acid) and gum arabic for the adsorption on the surface of the colloidal MnO_2 (the –OH groups of DL-malic acid and gum arabic are responsible for the adsorption—see later).

Rate dependence on [malic acid]

In order to see the effect of DL-malic acid on the rate constants, its concentration was varied from 16.0×10^{-4} to 64.0×10^{-4} mol dm^{-3} at [MnO_2] = 8.0×10^{-5} mol dm^{-3} and temperature = 30 °C (Table 1). The plots of k_{obs} versus [malic acid] are linear passing through the origin (Fig. 3), and the linear plots between log k_{obs} versus log [malic acid] yielded slopes of ca. 1.0 (r = 0.9895 (k_{obs1}), 0.9890(k_{obs2})). The reaction is, therefore, first-order with respect to [malic acid].

Rate dependence on [H^+]

Variation of the hydrogen ion concentration from 5.0×10^{-4} to 30.0×10^{-4} mol dm^{-3} employing perchloric acid at [MnO_2] = 8.0×10^{-5} mol dm^{-3} and [malic acid] = 16.0×10^{-4} mol dm^{-3} at 30 °C indicates that k_{obs} increases with [H^+] (Table 2). The plots of k_{obs} versus [H^+] are linear with positive intercepts on the y-axis, indicating acid-dependent as well as acid-independent routes (Fig. 4). A double-logarithmic plot of k_{obs1} and [H^+] was linear with a slope = 0.16, corresponding to a fractional-order dependence on [H^+].

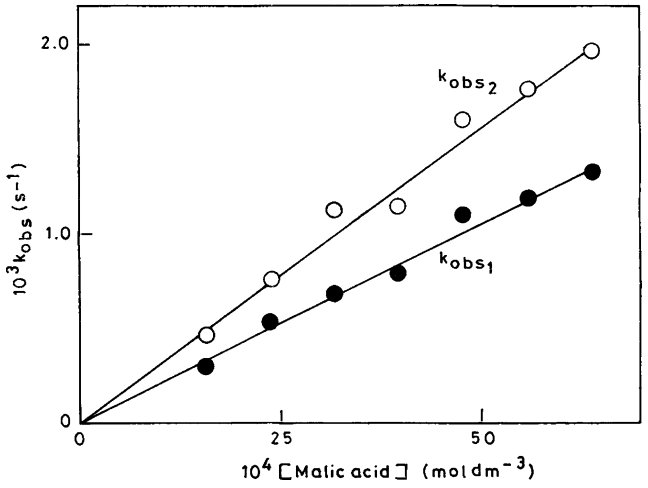

Fig. 3 Plots showing the effect of DL-malic acid on the pseudo-first-order rate constants. *Reaction condition*: $[MnO_2]$ = 8×10^{-5} mol dm^{-3}, temperature = 30 °C

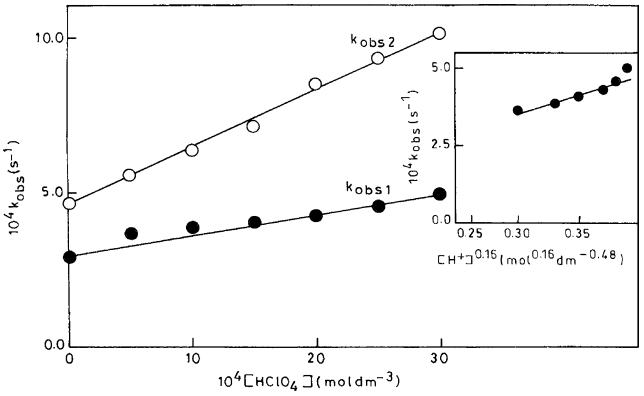

Fig. 4 Plots showing the effect of $HClO_4$ on the pseudo-first-order rate constants. *Reaction conditions*: $[MnO_2]$ = 8×10^{-5} mol dm^{-3}, [malic acid] = 16×10^{-4} mol dm^{-3}, temperature = 30 °C. *Inset* plots showing the effect of hydrogen ion concentration on the pseudo-first-order rate constant

Table 2 Pseudo-first-order rate constants for the oxidation of DL-malic acid by colloidal MnO_2

10^4 [$HClO_4$] (mol dm^{-3})	10^6 [Mn(II)] (mol dm^{-3})	10^4 k_{obs1} (s^{-1})	10^4 k_{obs2} (s^{-1})
0	0	2.9	4.6
5.0	0	3.6	5.5
10.0		3.8	6.3
15.0		4.0	7.1
20.0		4.2	8.5
25.0		4.5	9.3
30.0		4.9	10.1
0	5.0	3.8	6.5
	10.0	4.0	6.9
	20.0	4.5	7.4
	30.0	4.9	8.4
	40.0	5.4	9.4
	50.0	6.0	10.1

$[MnO_2]$ = 8×10^{-5} mol dm^{-3}, [malic acid] = 16×10^{-4} mol dm^{-3}, temperature = 30 °C

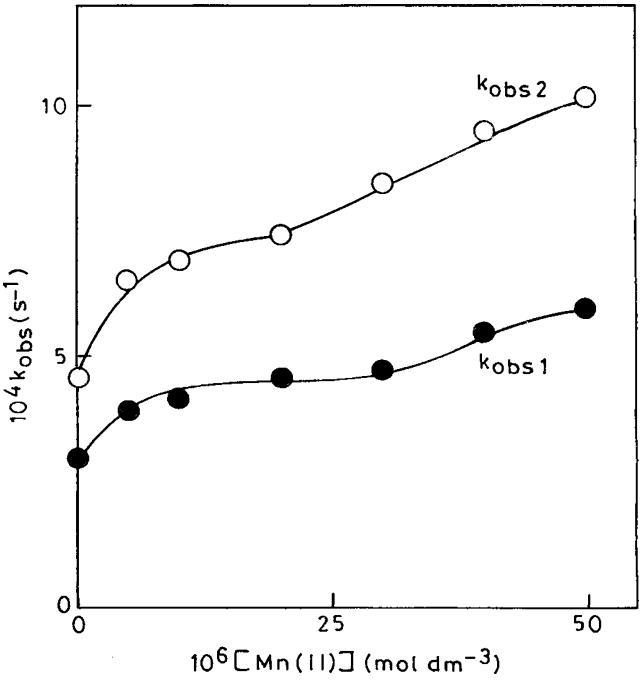

Fig. 5 Plots showing the effect of Mn(II) on the pseudo-first-order rate constants. *Reaction conditions*: $[MnO_2]$ = 8×10^{-5} mol dm^{-3}, [malic acid] = 16×10^{-4} mol dm^{-3}, temperature = 30 °C

Rate dependence on temperature

Effect of temperature was also studied within the range 25–40 °C at constant $[MnO_2]$ and [malic acid]. Activation parameters were obtained utilizing Arrhenius and Eyring equations by linear least-squares method. The results are given in Table 3.

The mechanism

The reaction under study is represented by Scheme 1, which corresponds to fast adsorption of DL-malic acid and hydrogen ions on the surface of MnO_2 with a one-step two-electron transfer process (Eq. 2) being the rate determining one. The H^+ – independence and H^+ – dependence can be explained on the basis of the mechanism.

I. H^+ — *independent*

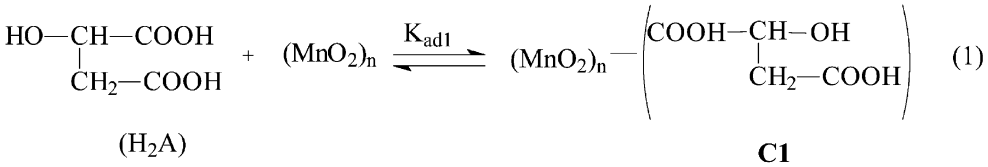

(1)

(H$_2$A) **C1**

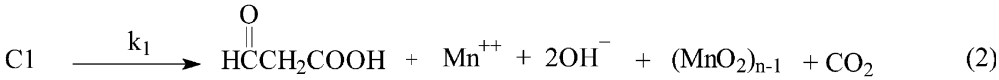

(2)

P1

II. H^+ — *dependent*

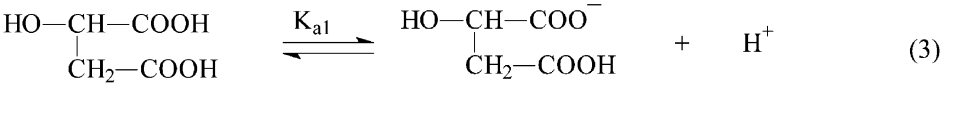

(3)

(HA^-)

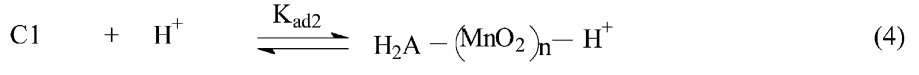

(4)

C2

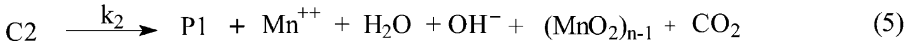

(5)

The mechanistic steps (Eqs. 1, 2, 3, 4, and 5) lead to the rate law (Eq. 6).

$$v = \frac{-\mathrm{d}[\mathrm{MnO_2}]}{\mathrm{d}t} = \frac{\left(k_1 K_{\mathrm{ad1}} + k_2 K_{\mathrm{ad1}} K_{\mathrm{ad2}} [\mathrm{H^+}]^2\right)[\mathrm{MnO_2}][\text{malic acid}]_T}{([\mathrm{H^+}] + K_{\mathrm{a1}})} \quad (6)$$

Table 3 Pseudo-first-order rate constants and activation parameters for the reaction of colloidal MnO_2 and DL-malic acid in the absence and presence of TX-100 (= 15.0×10^{-3} mol dm^{-3})

Temperature (mol dm^{-3})	Aqueous		TX-100	
	$10^4\ k_{\mathrm{obs1}}$ (s^{-1})	$10^4\ k_{\mathrm{obs2}}$ (s^{-1})	$10^4\ k_{\psi 1}$ (s^{-1})	$10^4\ k_{\psi 2}$ (s^{-1})
25	2.1	2.8	2.3	3.6
30	2.9	4.6	4.3	5.2
35	5.8	9.6	6.2	8.7
40	9.5	21.8	11.1	26.8
Activation parameters				
Ea (kJmol^{-1})	85	118	79	106
$\Delta H^{\#}$ (kJmol^{-1})	82	115	77	104
$\Delta S^{\#}$ (J K^{-1} mol^{-1})	−39	59	−55	37
$\Delta G^{\#}$ (kJ mol^{-1})	94	97	93	93

[MnO_2] = 8×10^{-5} mol dm^{-3}, [malic acid] = 16×10^{-4} mol dm^{-3}

and

$$k_{\mathrm{obs1}} = \frac{\left(k_1 K_{\mathrm{ad1}} + k_2 K_{\mathrm{ad1}} K_{\mathrm{ad2}} [\mathrm{H^+}]^2\right)[\text{malic acid}]_T}{([\mathrm{H^+}] + K_{\mathrm{a1}})}. \quad (7)$$

The reaction has a fractional-order dependence in [$HClO_4$] (under the kinetic conditions of [$HClO_4$] ≥5.0×10^{-4} to 30.0×10^{-4} mol dm^{-3}) and, it is, therefore, apparent that k_1 (acid-independent path) can be neglected in comparison to k_2 (acid-dependent path). By introducing this approximation, the rate law (Eq. 7) is thus reduced to Eq. 8, which clearly explains the fractional-order dependence on [H^+].

$$k_{\mathrm{obs1}} = \frac{\left(k_2 K_{\mathrm{ad1}} K_{\mathrm{ad2}} [\mathrm{H^+}]^2\right)[\text{malic acid}]_T}{([\mathrm{H^+}] + K_{\mathrm{a1}})}. \quad (8)$$

Rate dependence on [Mn(II)]

The rate constants, obtained as a function of initially added [Mn(II)] with other variables remaining constant ([MnO_2] = 8.0×10^{-5} mol dm^{-3} and [malic acid] = 16.0×10^{-4} mol dm^{-3} at 30 °C), were found to increase with increasing [Mn(II)] (Table 2). The k_{obs}—[Mn(II)]

profiles show sigmoid dependence of the reaction pathways on [Mn(II)] establishing Mn(II) as the autocatlyst. Further, plots of log k_{obs} versus log[Mn(II)] resulted in two straight portions with slopes of ca. 0.1 and 0.3, suggesting that the reaction is zero-and fractional-order with respect to [Mn(II)] at lower and higher concentrations. In the presence of Mn(II), Scheme 1 is, therefore, modified as Scheme 2

$$(MnO_2)_n + Mn(II) \xrightarrow{\text{pathI}} (MnO_2)_{n-1} + Mn(III) \quad (9)$$

$$(MnO_2)_n + \text{DL-malic acid} \xrightarrow{\text{pathII}} (MnO_2)_{n-1} + Mn(II) + \text{other products} \quad (10)$$

In the presence of Mn(II) there is a competition between the DL-malic acid and Mn(II) to react with the colloidal MnO_2. Thus, we may conclude that the values of rate constants (Table 2, see the above discussion on Mn(II) effect or Scheme 2) are the sum of the paths I and II. As the contribution of path I cannot be completely ruled out, the exact dependence of k_{obs1}/k_{obs2} on [Mn(II)] cannot be predicted. (In addition, involvement of intermediates/products is yet another possibility for the observed autocatalysis.) In order to observe the formation of Mn(III) species (see Eq. 9), some experiments monitoring absorbance at 470 nm (where Mn(III) is the only absorbing species [19]) were also performed but we failed to observe any build up of Mn(III) during the course of the reaction.

To see the role of surfactants (anionic, cationic or nonionic), attempts were made to carry out the oxidation reaction under different experimental conditions, i.e., reaction mixture + SDS, reaction mixture + CTAB, and reaction mixture + TX-100. The values of rate constants (k_Ψ, s^{-1}) are summarized in Tables 1, 3 and 4. Preliminary observations showed that a reaction mixture containing [MnO_2] (= 8×10^{-5} mol dm^{-3}), [malic acid] (= 16×10^{-4} mol dm^{-3}) and cationic micelles of CTAB became turbid due to flocculation. CTAB micelles have positive charge on their head group, whereas colloidal MnO_2 has negative charge [20]. The anionic SDS surfactant neither catalyzed nor inhibited the oxidation reaction (Table 4). The observation is not unexpected; anionic micelles, simply based on electrostatic considerations, will repel the oxidant (colloidal MnO_2) keeping the bulk reaction unaffected.

The k_Ψ–[TX-100] profiles show positive catalysis (Fig. 6), which may be explained in terms of increasing solubilization and association or adsorption of the reactive species of DL-malic acid and MnO_2 with increase in the [TX-100] that reaches a limiting value. Hence, a rate maximum is observed. Further increase in [TX-100] results in increase in the adsorption of the TX-100 on the colloidal MnO_2. This would hinder the adsorption/association of DL-malic acid with colloidal MnO_2 with the concomitant decrease in the effective concentration of DL-malic acid at the surface of the colloidal MnO_2 particles. This effect is probably operative at higher [TX-100] and seems responsible for decrease in k_Ψ (Fig. 6). Thus we may conclude that the increase–decrease behaviour of k_Ψ depends upon the concentration of adsorbed TX-100 and DL-malic acid.

The pseudo-first-order rate constants for the oxidation of DL-malic acid by colloidal MnO_2 were also obtained over a range of concentrations of MnO_2, DL-malic acid and temperature in the presence of TX-100 (= 15.0×10^{-3} mol dm^{-3}). The order with respect to MnO_2 and DL-malic acid was first. These observations undoubtedly show that the reaction mechanism in the presence of nonionic surfactant TX-100 remains the same as that in the homogeneous aqueous medium. A lower value of activation energy in the presence of TX-100 (Table 3) clearly suggests the surfactant's catalytic role.

In order to explain the micellar catalytic effect on the oxidation, an attempt has been made to employ the mathematical model proposed by Tuncay et al. [3] (Eqs. 11 and 12)

$$\log k_{\psi 1} = a \log[\text{TX} - 100] - b, \quad (11)$$

$$\log k_{\psi 2} = a' \log[\text{TX} - 100] - b', \quad (12)$$

where $k_{\Psi 1}$ and $k_{\Psi 2}$ are pseudo-first-order rate constants for the nonautocatalytic and autocatalytic pathways, respectively, (a and b being empirical constants). The

Table 4 Pseudo-first- order rate constants for the oxidation of DL-malic acid by colloidal MnO_2

10^3 [TX-100] (mol dm^{-3})	10^4 $k_{\psi 1}$ (s^{-1})	10^4 $k_{\psi 2}$ (s^{-1})
0.0	2.9 (2.9, 2.9)[a]	4.6 (4.5, 4.6)[a]
5.0	3.8	4.9
10.0	4.2	5.1
15.0	4.2	5.2
20.0	4.6	5.4
30.0	3.5	4.5
40.0	3.3	4.4
50.0	3.2	4.3

[MnO_2] = 8×10^{-5} mol dm^{-3}, [malic acid] = 16×10^{-4} mol dm^{-3}, temperature = 30°C

[a]The values quoted in parenthesis were obtained, respectively at [SDS] = 4×10^{-3} and 20×10^{-3} mol dm^{-3}

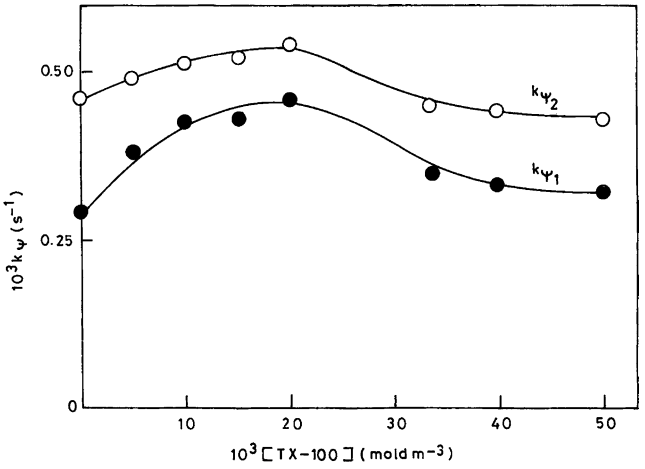

Fig. 6 Plots showing the effect of TX-100 on the pseudo-first-order rate constants. *Reaction conditions*: [malic acid] = 16×10^{-4} mol dm^{-3}, [MnO_2] = 8×10^{-5} mol dm^{-3}, temperature = 30 °C

above equations predict that the plots of log k_Ψ versus log [TX-100] should be linear with slopes (a and a') and intercepts (b and b'). When the data were fitted, clear linear plots resulted, Fig. 7a, indicating that the model is adequate to explain the present reaction. The values of a = 0.1197, b = 3.1385, a' = 0.0653 and b' = 3.1593 were obtained from Fig. 7a plots.

Furthermore, the following equations were also suggested [3]:

$$\frac{1}{(k_{\psi 1} - k_{\text{obs1}})} = x + \frac{y}{[\text{TX} - 100]}, \tag{13}$$

$$\frac{1}{(k_{\psi 2} - k_{\text{obs2}})} = x' + \frac{y'}{[\text{TX} - 100]}. \tag{14}$$

The plots of the left-hand sides of Eqs. 13 and 14 versus 1/[TX-100] were linear, making intercepts on the y-axis (Fig. 7b), thus satisfying validity of the equations. Values of x = 0.33×10^2 s, y = 4,452.10 mol dm^{-3} s, $x' = 1.34\times10^2$ s, and y' = 6,450.79 mol dm^{-3} s for $k_{\Psi 1}$ and $k_{\Psi 2}$ were calculated from the intercepts and slopes of Fig. 7b.

As the reaction is found to be catalyzed by TX-100, the question is: what could be the role of this nonionic surfactant? The main body of nonionic TX-100 is composed of saturated alkyl and polyoxyethylene chains. The rates of chemical reactions being affected by surfactants are mainly due to localization/compartmentalization, pre-orientational, polarity and counterion effects. The exact reaction site cannot be proposed because the micellar pseudo-phase is regarded as a microenvironment having varying degrees of water activity, polarity and hydrophobicity. The activity of water at the surface is not different from water activity in

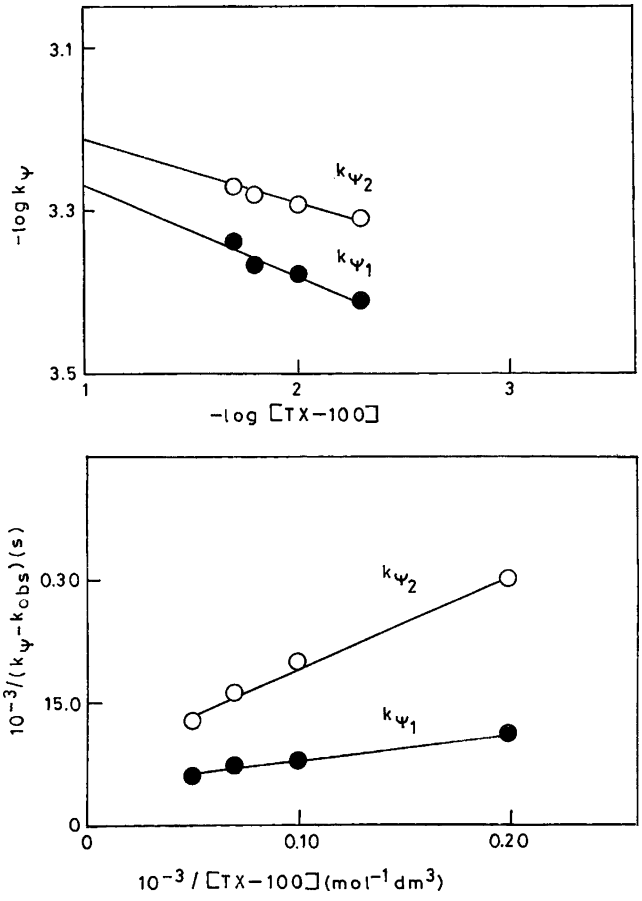

Fig. 7 Plots of log k_ψ versus log[TX-100] (**a**) and ($1/k_\psi$ − k $_{obs}$) versus 1/[TX-100] (**b**). *Reaction conditions*: [malic acid] = 16×10^{-4} mol dm^{-3}, [MnO_2] = 8×10^{-4} mol dm^{-3}, temperature = 30 °C. The data belong to the part upto which the effect of TX-100 was catalytic (cf. Fig. 6)

the aqueous pseudo-phase. Therefore, at present, the localization of MnO_2 and DL-malic acid can be considered. Three important factors, namely, electrostatic, hydrophobic and hydrogen bonding seem to play an important role in bringing the reactants (MnO_2 and DL-malic acid) together. As far as the role of nonionic TX-100 is concerned, any type of electrostatic interaction is not possible. Also, the hydrophobicity of DL-malic acid is diminished due to the presence of two –COOH groups. Thus, only one factor, namely hydrogen bonding, is left for the catalytic role of TX-100. Therefore, the hydrogen bonding between MnO_2 sols and polyethylene oxygen of TX-100 seems responsible for the adsorption of TX-100 on the surface of the colloidal MnO_2. Hydrogen bonding between the –COOH and –OH groups of DL-malic acid and the oxygen of the polyoxyethylene chain of TX-100 may also take place. As a result, TX-100 helps in bringing the MnO_2 and DL-malic acid closer, which may orient in a manner suitable for the redox reaction followed by rearrangement of TX-100

molecules. The formation of a complex-type species between the MnO_2 and DL-malic acid is a characteristic feature of the mechanism of adsorption reaction. Therefore, the associated MnO_2 and DL-malic acid with TX-100 (through hydrogen bonding) seemingly facilitate formation of the complex (C1/C2) and this might be the main role of nonionic TX-100 surfactant toward catalysis.

References

1. Perez-Benito JF, Arias C (1992) J Colloid Interface Sci 149:92
2. Perez-Benito JF, Arias C, Amat E (1996) J Colloid Interface Sci 177:288
3. Tuncay M, Yuce N, Arlkan B, Gokturk S (1999) Colloids Surf A Physicochem Eng Aspects 149:279
4. Kabir-ud-Din, Fatma W, Khan Z (2004) Colloids Surf A Physicochem Eng Aspects 234:159
5. Khan Z, Raju, Akram M, Kabir-ud-Din (2004) Int J Chem Kinet 36:359
6. Khan MN (1995) J Mol Cata 93:102
7. Khan MN, Arfin Z (1996) J Colloid Interface Sci 9:180
8. Khan MN (1997) Colloids Surf A Physicochem Eng Aspects 127:211
9. Bunton CA (1997) J Mol Liq 72:231
10. Bunton CA, Gillitt ND (2002) J Phys Org Chem 15:29
11. Kabir-ud-Din, Morshed AMA, Khan Z (2002) J Carbohydr Res 337:1573
12. Kabir-ud-Din, Morshed AMA, Khan Z (2003) Oxidation Comm 26:59
13. Hasan F, Rocek J (1972) J Am Chem Soc 94:9073
14. Hasan F, Rocek J (1975) J Am Chem Soc 96:127
15. Kabir-ud-Din, Hartani K, Khan Z (2000) Transition Met Chem 25:487
16. Kabir-ud-Din, Iqubal SMS, Khan Z (2004) Inorg React Mech (in press)
17. Tompkins FC (1942) Trans Faraday Soc 38:131
18. Wiberg KB, Stewart R (1955) J Am Chem Soc 77:1786
19. Macartney DH, Sutin N (1985) Inorg Chem 24:3403
20. Perez-Benito JF, Brillas E, Pouplana R (1989) Inorg Chem 28:390